# Thin water film around a cable subject to wind

C. Lemaitre[1], P. Hémon[1] & E. de Langre[1]

ABSTRACT: *Cables of cable-stayed bridges can experience rain-wind induced vibrations. This instability involves lower frequencies and higher amplitudes than classical vortex induced vibrations. Furthermore, this is a wind velocity restricted phenomenon unlike galloping. When flowing along the cables, the water gathers near the separation points to form one or two rivulets. Former studies which have described the coupling between the rivulets motion and the cable motion, assume the existence of the rivulet. In this paper, we address the conditions for the rivulets to form. A two-dimensional model is developed within the lubrication theory. It describes the evolution of a thin film submitted to gravity, surface tension, wind and motion of the cylinder. Numerical simulations show the appearance of the rivulets that are reputedly responsible for the instability.*

## 1 INTRODUCTION

On cable-stayed bridges, inclined cables connect the pylons to the deck, Figure 1. The cables can experience vibrations which are due both to the presence of rain and wind (rain-wind induced vibrations, RWIV). First reported by Hikami & Shiraishi (1988), this particular type of instability happens by moderate rain and rather low wind speed, typically $10 \ m/s$ and vibrations stop when the rain stops. Unlike the instabilities due to the sole wind, RWIV are not fully understood. Observations in full-scale as well as experiments conducted in wind tunnels show that only cables declining in the direction of the wind are concerned by RWIV. The vibrations are generally crosswind, Hikami & Shiraishi (1988). The involved amplitudes of vibrations are higher and the frequencies lower than those of vortex-induced vibrations, Hikami & Shiraishi (1988). This is furthermore a velocity restricted phenomenon, unlike the galloping of Den Hartog (1985), for which there is no maximum wind speed.
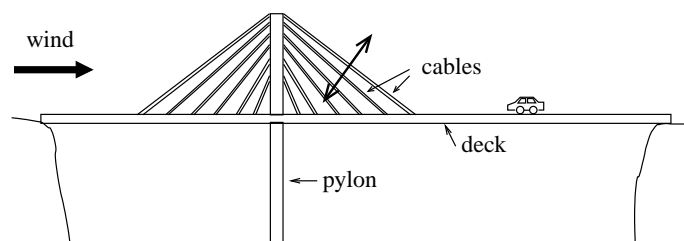


Figure 1 Cable-stayed bridge. Only cables declining in the wind direction undergo RWIV.

In unstable cases, the water flows around the cable and one to two rivulets form near the separation points of the air-flow around the dry cylinder, Bosdogianni & Olivari (1996). The two rivulets oscillate circumferentially, at the same frequency as the cable motion, Hikami & Shiraishi (1988). Some sine waves travel along the upper rivulet whereas the bottom rivulet stays rectilinear, Xu et al. (2002) Authors agree that the presence of the upper rivulet is required for the instability to take place, Matsumoto et al. (1995) and Bosdogianni & Olivari (1996). It is unclear however whether the motion of the upper rivulet is necessary or not. Experiments by Verwiebe & Ruscheweyh (1998) and Flamand (1995) tend to show that an artificial rivulet fixed on the cylinder, exposed to a RWIV-like wind does not provoke instability. On the contrary, Bosdogianni & Olivari (1996) and Matsumoto et al. (1995) observe vibrations of the cable in similar experiments.

Former models such as the one of Yamaguchi (1990), assume the existence of the upper rivulet. In this article, the conditions for the appearance of the rivulets are investigated. A new model is presented in section 2 that describes the evolution of a thin water film around a moving cable subject to wind. Numerical results from this model are discussed in section 3.

## 2 MODEL

This section presents a new two-dimensional model based on lubrication theory that describes the behaviour of a thin water film in cylindrical configuration, evolving under the effect of gravity, surface tension, wind and motion of the support.

[1] Ph.D. Cécile Lemaitre, Dr. Pascal Hémon, Ass. Prof. Emmanuel de Langre,
Department of mechanics: LadHyX, CNRS-Ecole Polytechnique, 91128 Palaiseau, France,
e-mail `cecile.lemaitre@ladhyx.polytechnique.fr`
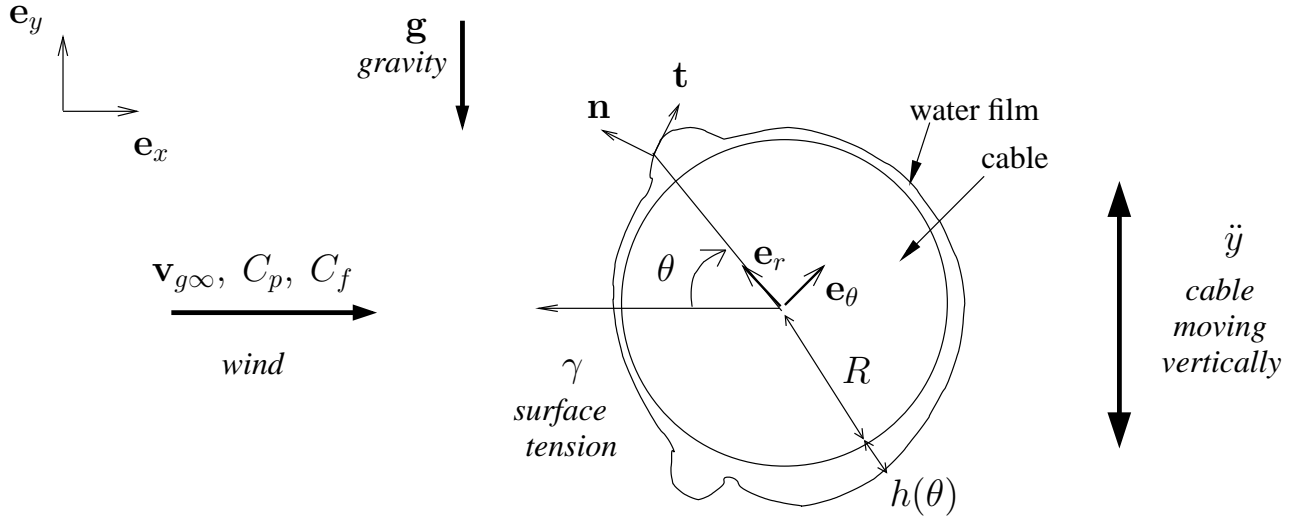
Figure 2 Water film around a cable subject to gravity, surface tension and swept by wind.

Reisfeld & Bankoff (1992) derived the equations for a thin film surrounding a cylinder, subject to gravity and surface tension. Following a similar approach we modelled the actions of wind and cable motion on the film, by considering them as an external forcing.

### 2.1 Geometry and notations

A thin film of thickness $h(\theta)$ is considered, surrounding a horizontal cylinder of radius $R$, Figure 2. The film is assumed to be continuous: there is no dewetting and the quantity of matter is constant (no drop break off). It has a characteristic thickness $h_o$. It is subject to gravity

$$\mathbf{g} = -g\mathbf{e}_y \tag{1}$$

and to a homogeneous surface tension, $\gamma$ independent of $\theta$. If an inclined cylinder were considered instead of a horizontal one, the effective gravity would be lower. A wind blows from the left with a horizontal upstream velocity

$$\mathbf{v_{g\infty}} = v_{g\infty}\mathbf{e}_x \tag{2}$$

and produces pressure and friction coefficients $C_p(\theta)$ and $C_f(\theta)$ at each point on the film surface. As the rain-wind induced vibrations are mostly transverse to the wind direction, the cable is chosen to undergo a vertical motion. Its displacement, $\mathbf{y} = y\mathbf{e}_y$, has a characteristic amplitude $y_o$ and its evolution in time, with a characteristic time $T_y$, is described by a functional $f$:

$$y(t) = y_o f(t/T_y) \tag{3}$$

The acceleration of the cable produces an added gravity that depends on time:

$$\mathbf{g}_a = -\ddot{y}\mathbf{e}_y = -\frac{y_o}{T_y^2}f''\left(\frac{t}{T_y}\right)\mathbf{e}_y \tag{4}$$

### 2.2 Navier-Stokes and boundary conditions

The Navier-Stokes equations are written in the water film:

$$\begin{cases} \rho\dfrac{D\mathbf{v}}{Dt} = \rho\left(\mathbf{g} + \mathbf{g}_a\right) - \nabla p + \mu\Delta\mathbf{v} \\ \nabla.\mathbf{v} = 0 \end{cases} \tag{5}$$

where $\mathbf{v}$ is the velocity field in the water film, $\rho$ is the water density, $p$ is the pressure in the film and $\mu$ is the dynamic viscosity of water. These equations are written in cylindrical coordinates on the local frame $(\mathbf{e}_r, \mathbf{e}_\theta)$. In this frame, the position of a water particle is expressed $\mathbf{r} = r\mathbf{e}_r$ ($R \leq r \leq R+h$) and its velocity decomposes into $\mathbf{v} = u\mathbf{e}_r + v\mathbf{e}_\theta$. At each point of the water/air interface, the normal and tangential vectors read:

$$\mathbf{t} = \frac{1}{N}\left(\frac{h_\theta}{r}\mathbf{e}_r + \mathbf{e}_\theta\right)$$

$$\mathbf{n} = \frac{1}{N}\left(\mathbf{e}_r - \frac{h_\theta}{r}\mathbf{e}_\theta\right) \tag{6}$$

$$N = \left(1 + \frac{h_\theta^2}{r^2}\right)^{1/2}.$$

The subscript $\theta$ indicates differentiation in space; the subscripts $t$ and $T$ that will come up later on indicate differentiation in time.

The associated boundary conditions are:
(i) the water particles do not slip on the cable:

$$u = v = 0 \tag{7}$$

(ii) the water/air interface is a material surface that no water particle can cross. The normal velocity of a water particle on the interface is thus equal to the normal velocity of the interface, which is translated into:

$$u = h_t + \frac{v}{r}h_\theta \tag{8}$$

where the subscripts $t$ (iii) the jump in the normal shear stress is balanced by the surface tension:

$$
\begin{cases}
\mathbf{n}.(\sigma_g - \sigma).\mathbf{n} = \mathcal{K}\gamma \quad , \\
\mathbf{t}.(\sigma_g - \sigma).\mathbf{n} = 0
\end{cases}
\tag{9}
$$

where $\sigma_g$ and $\sigma$ are the Cauchy stress tensors of the gas and the water respectively, $\mathcal{K}$ is the curvature of the water/air interface, $\gamma$ is the surface tension and $\mathbf{n}$ is the normal vector at the interface. The stress tensor in water is expressed by

$$
\sigma = -p\mathbf{I} + 2\mu\mathbf{D} \quad , \tag{10}
$$

where $\mathbf{I}$ is the identity tensor and the deformation rate tensor $\mathbf{D}$ is defined by:

$$
\mathbf{D} = \frac{1}{2}\left[\nabla\mathbf{v} + (\nabla\mathbf{v})^T\right] \tag{11}
$$

The curvature $\mathcal{K}(\theta)$ of the free surface of the film is:

$$
\begin{aligned}
\mathcal{K}(\theta) &= \nabla.\mathbf{n} \\
&= \frac{(R+h)^2 + 2h_\theta^2 - (R+h)h_{2\theta}}{[(R+h)^2 + h_\theta^2]^{3/2}}
\end{aligned}
\tag{12}
$$

The action of the wind is introduced through the expression of the air stress tensor:

$$
\sigma_g = -p_g(\theta)\mathbf{I} + \tau_g \quad , \tag{13}
$$

where $\tau_g$ is the viscous stress tensor of air.

### 2.3 Lubrication and dimensionless equations

The assumptions of lubrication are now made:
a) The Reynolds number based on the film thickness close to one: $Re_h = h_o v/\nu \approx 1$.
b) The film is thin compared to the cable radius: $h_o \ll R$.
c) The film thickness $h$ evolves 'slowly' with $\theta$: $\partial_\theta h \ll R$.
As a consequence, the following dimensionless variables are defined:

$$
\begin{aligned}
U = \frac{R}{\nu}u \quad V = \frac{h_o}{\nu}v \quad T = \frac{\nu}{Rh_o}t \\
P = \frac{h_o^3}{\rho\nu^2 R}p \quad \xi = \frac{r-R}{h_o} \quad H = \frac{h}{h_o}
\end{aligned}
\tag{14}
$$

They are based on viscosity scales. A dimensionless gas pressure is defined with the pressure coefficient divided by its maximum value:

$$
C_p = \frac{p_g}{\frac{1}{2}\rho_g v_{g\infty}^2} \quad ; \quad \overline{C}_p = \frac{C_p}{max(C_p)} \tag{15}
$$

In the same way, the reduced gas friction is formed with the normalised friction coefficient $\overline{C}_f$:

$$
C_f = \frac{\mathbf{t}.\tau_g.\mathbf{n}}{\frac{1}{2}\rho_g v_{g\infty}^2} \quad ; \quad \overline{C}_f = \frac{C_f}{max(C_f)} \tag{16}
$$

These variables are assumed to be of order magnitude one.

When putting the Navier-Stokes and the boundary condition equations in a non dimensional form, the small parameter $\varepsilon = h_o/R$ and the following dimensionless numbers appear:

$$
\begin{aligned}
G &= \frac{gh_o^3}{3\nu^2} \qquad S = \frac{\gamma h_o^4}{3\rho\nu^2 R^3} \\
\mathcal{A} &= \frac{y_o h_o^3}{3\nu^2 T_y^2} \quad \Omega_y = \frac{2\pi R h_o}{\nu T_y} \\
\mathcal{P} &= \frac{\rho_g v_{g\infty}^2 h_o^3 max(C_p)}{6\rho\nu^2 R} \\
\mathcal{F} &= \frac{\rho_g v_{g\infty}^2 h_o^2 max(C_f)}{4\rho\nu^2}
\end{aligned}
\tag{17}
$$

The numbers $G$, $S$, $\mathcal{A}$, $\mathcal{P}$ and $\mathcal{F}$ compare the actions of gravity, surface tension, cable acceleration, air pressure and air friction respectively, to the action of water viscosity. The reduced pulsation $\Omega_y$ compares the cable motion characteristic time to the viscous time.

Only the terms of leading order in $\varepsilon$ are kept to yield the linearised Navier-Stokes equations:

$$
\begin{cases}
P_\xi = 0 \\
-3\left(G + \mathcal{A}f''\left(\frac{\Omega_y}{2\pi}T\right)\right)\cos\theta \\
\qquad\qquad - P_\theta + V_{\xi\xi} = 0 \\
U_\xi + V_\theta = 0
\end{cases}
\tag{18}
$$

and the linearised boundary condition equations:

$$
\begin{cases}
U|_{\xi=0} = V|_{\xi=0} = 0 \\
U|_{\xi=H} = H_T + V|_{\xi=H}H_\theta \\
-3\mathcal{P}\,\overline{C}_p + P|_{\xi=H} = 3S(\frac{1}{\varepsilon} - H - H_{\theta\theta}) \\
2\mathcal{F}\,\overline{C}_f - (V_\xi)\,|_{\xi=H} = 0
\end{cases}
\tag{19}
$$

Equation (18)-3 is integrated between $\xi = 0$ and $\xi = H$; the condition $U|_{\xi=0} = 0$ is then used:

$$
U = -\int_{\xi=0}^{H} V_\theta d\xi \tag{20}
$$

This is injected into equation (19)-2 and condensed into:

$$
H_T + \left[\int_{\xi=0}^{H} V d\xi\right]_\theta = 0 \tag{21}
$$

The pressure in the water film $P$ is independent of $\xi$ (equation (18)-1). The expression of $P$ given by equation (19)-3 is thus valid in the whole film and is injected into equation (18)-2:

$$V_{\xi\xi} = 3\left(G + \mathcal{A}f''\right)\cos\theta$$
$$+ \left[3S(\frac{1}{\varepsilon} - H - H_{2\theta}) + 3\mathcal{P}\overline{C}_p\right]_\theta \tag{22}$$

This last equation is integrated twice with respect to $\xi$ and equations (19)-1 and (19)-4 are used to get:

$$V = \frac{3}{2}\Big[\left(G + \mathcal{A}f''\right)\cos\theta - S(H_\theta + H_{3\theta})$$
$$+ \mathcal{P}(\overline{C}_p)_\theta\Big]\left(\xi^2 - 2H\xi\right) + 2\mathcal{F}\overline{C}_f\xi \tag{23}$$

This expression of the azimuthal velocity is replaced in equation (21) and we finally obtain:

$$H_T - \left[G + \mathcal{A}f''\left(\Omega_y T/2\pi\right)\right]\left\{H^3\cos\theta\right\}_\theta$$
$$+ S\left\{(H_\theta + H_{3\theta})H^3\right\}_\theta \tag{24}$$
$$- \mathcal{P}\left\{(\overline{C}_p)_\theta H^3\right\}_\theta + \mathcal{F}\left\{\overline{C}_f H^2\right\}_\theta = 0$$

This is an equation of conservation of the thickness $H$, with a flux $g$:

$$H_T + g_\theta = 0$$
$$g = \Big[-\left(G + \mathcal{A}f''\right)\cos\theta + S(H_\theta + H_{3\theta}) \tag{25}$$
$$- \mathcal{P}(\overline{C}_p)_\theta\Big]H^3 + F\overline{C}_f H^2$$

For $\mathcal{A} = 0$, $\mathcal{P} = 0$ and $\mathcal{F} = 0$ equation (24) is the same as Reisfeld & Bankoff (1992), equation (4.16). The shape of the air friction term is consistent with equation (2.31) of Oron et al. (1997) for a thin film on a plane.

## 3 RESULTS

In this section, equation (24) is solved in the parameter range of the rain-wind induced vibrations. It is assumed here that the wind load on the film is the same as the wind load around the dry cable. The values of the wind load around a dry cable are supposed to apply along the film local normal and tangent vectors of the water film. The Reynolds number based on the cable diameter in RWIV conditions is:

$$Re_g = \frac{2Rv_{g\infty}}{\nu_g} \approx 10^5 \tag{26}$$

where $\nu_g$ is the air viscosity, the typical cable radius being $R = 0.1\ m$ and the typical wind speed $v_{g\infty} = 10\ m/s$. Achenbach (1968) measured the pressure and friction distribution produced by an air

flow on a smooth cylinder oriented in the cross-flow direction. His values at the same Reynolds number are used for the computations, Figure 3.
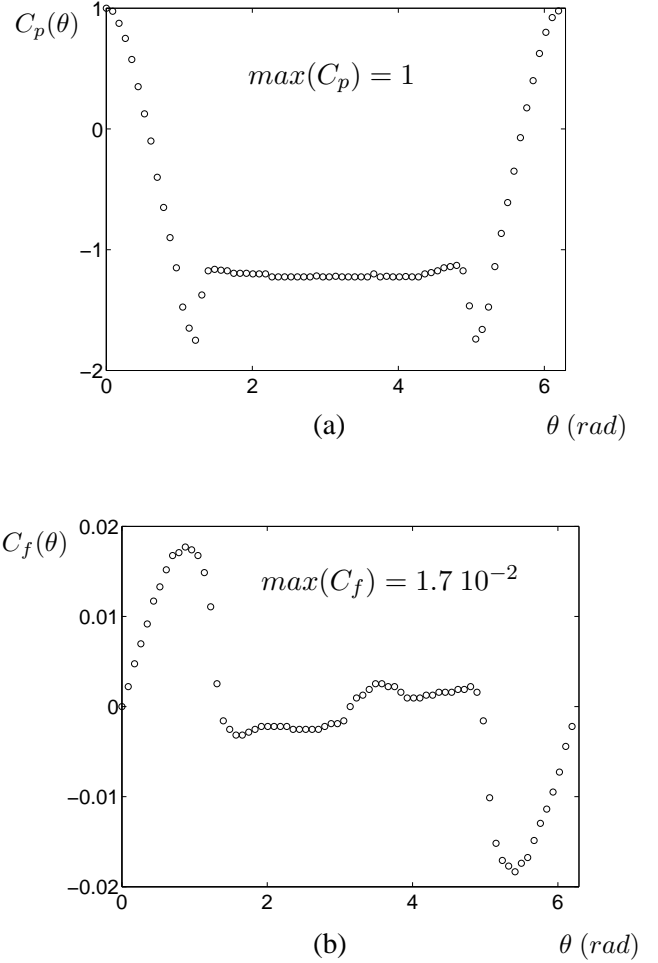


Figure 3 Distribution of the wind load around a smooth dry cylinder at $Re_g = 10^5$, measured by Achenbach (1968).(a) Pressure coefficient, (b) Friction coefficient.

The control parameters of equation (24) have been computed for experiments from the literature, Table 1.

Table 1 Parameter values for literature experiments. [1]-1: Hikami & Shiraishi (1988), full-scale observation; [1]-2: Hikami & Shiraishi (1988), wind tunnel experiment; [2]: Flamand (1995); [3]: Matsumoto et al. (1995).

| Authors | [1]-1 | [1]-2 | [2] | [3] |
|---|---|---|---|---|
| $\varepsilon$ | $1.4\ 10^{-2}$ | $1.4\ 10^{-2}$ | $5.6\ 10^{-3}$ | $1.2\ 10^{-2}$ |
| $G$ | $3.3\ 10^3$ | $3.3\ 10^3$ | $3.0\ 10^2$ | $3.3\ 10^3$ |
| $S$ | $7.1\ 10^{-2}$ | $7.1\ 10^{-2}$ | $1.9\ 10^{-3}$ | $4.0\ 10^{-2}$ |
| $\mathcal{A}$ | $2.1\ 10^2$ | $3.7\ 10^1$ | $5.5$ | $1.8\ 10^1$ |
| $\Omega_y$ | $8.8\ 10^2$ | $4.4\ 10^2$ | $2.3\ 10^2$ | $3.0\ 10^2$ |
| $\mathcal{P}$ | $3.5\ 10^2$ | $3.5\ 10^2$ | $2.8\ 10^1$ | $2.4\ 10^2$ |
| $\mathcal{F}$ | $6.4\ 10^2$ | $6.4\ 10^2$ | $1.3\ 10^2$ | $5.3\ 10^2$ |

It is remarkable that the pressure number $\mathcal{P}$ and the friction number $\mathcal{F}$ are the same order of magnitude. The friction of air shall have a major effect on the dynamics of the film.

Equation (24) is a partial differential equation of the fourth order that is non linear with non constant coefficients. It is thus not solvable analytically and numerical computations are needed. The computations are carried out with a pseudo-spectral method: a Fourier spectral method in space and an Adams-Bashforth scheme of the fourth order in time. The figure 4 shows a resolution of equation (24) with a static cable, $\mathcal{A} = 0$ and the other parameters computed from Flamand (1995). At the initial time, the thickness of the film is constant in space, $H(T = 0) = 1$. The resolution in space is of $N_x = 128$ points and the time step is $dT = 10^{-6}$.

Two water bulges form at the top and at the bottom of the cylinder, bidimensional traces of the rivulets. They are located in the neighbourhood of the separation points that the air flow would present if it were flowing around the dry cylinder. Their size increases until the lubrication assumptions get violated. Under the effect of gravity the bottom protuberance grows faster than the upper one. As observed by Reisfeld & Bankoff (1992), a cusp is bound to appear at $\theta = 3\pi/2$ under gravity action, but its formation is slower than the dynamics of formation of the rivulets.
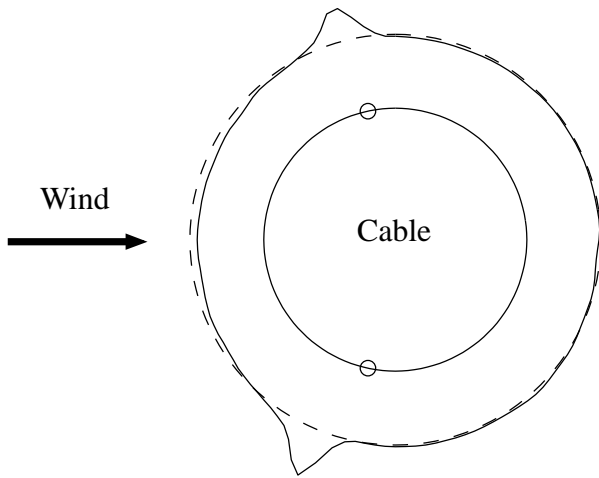


Figure 4 Numerical solution of equation (24) starting from a homogeneous film, submitted to gravity, surface tension and wind. The cable radius is $R = 0.08 \, m$. The film thickness is represented one hundred times as large. $(--)$ Film at $t = 0 \, s$ ; $(-)$ Film at $t = 3.6 \times 10^{-3} \, s$ ; $(o)$ Separation points of the air flow around the dry cable

In order to study the relative effect of friction compared to pressure, the two following artificial cases are considered:
* A film of initial constant thickness is submitted to surface tension $(S = 1.9 \times 10^{-3})$ and pressure $(\mathcal{P} = 2.8 \times 10^1)$, the other terms of equation (24) being set to zero $(G = 0, \mathcal{A} = 0$ and $\mathcal{F} = 0)$.
* Another computation is done where only the terms due to surface tension $(S = 1.9 \times 10^{-3})$ and friction $(\mathcal{F} = 1.3 \times 10^2)$ are retained $(G = 0, \mathcal{A} = 0$ and

$\mathcal{P} = 0)$.
The same numerical methods as above are implemented $(N_x = 128, dT = 10^{-6})$ to give the results which are presented on Figure 5.
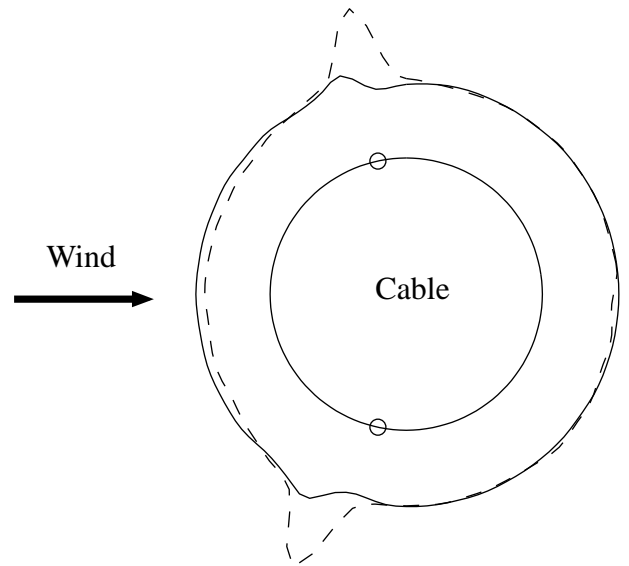


Figure 5 Comparison of pressure and friction actions. The cable radius is $R = 0.08 \, m$. The films are represented one hundred times as large at $t = 6.3 \times 10^{-3} \, s$ . $(-)$ Film evolving under pressure and surface tension only; $(--)$ Film evolving under friction and surface tension only; $(o)$ Separation points of the air flow around the dry cable

Both the computations show the appearance and growth of two rivulets in the region of the separation points. The rivulets generated by friction grow faster and larger than those generated by pressure. Moreover, the rivulets due to pressure are located slightly upstream the friction generated rivulets. The action of friction appears to dominate the rivulet generation.

## 4 CONCLUSION

We have presented here a model that describes for the first time the evolution of a water film around a cylinder under the action of wind and cylinder motion. This model recovers well the appearance of the two water rivulets that are said to be responsible for rain-wind induced vibration of cables of cable-stayed bridges. In accordance with experimental observations, the rivulets form in the region of the separation points of the air flow around the dry cable under the combined effect of air pressure and friction. The friction is found to play a major role in the generation of the rivulets. The existence of solutions at long times to the problem is currently investigated.

## 5 REFERENCES

Achenbach, E. (1968) Distribution of local pressure and skin friction around a circular cylinder in a cross-flow

up to $Re = 5 \times 10^6$. *Journal of Fluid Mechanics*, 34, 4, pp. 625-639.

Bosdogianni, A. & Olivari, D. (1996) Wind- and rain-induced oscillations of cables of stayed bridges. *Journal of Wind Engineering and Industrial Aerodynamics*, 64, pp. 171-185.

Den Hartog, J.P. (1985) *Mechanical vibrations. Dover Publications, Inc. New-York*, pp. 299-304.

Flamand, O. (1995) Rain-wind induced vibration of cables. *Journal of Wind Engineering and Industrial Aerodynamics*, 57, pp. 353-362.

Hikami, Y. & Shiraishi, N. (1988) Rain-wind induced vibrations of cables in cable-stayed bridges. *Journal of Wind Engineering and Industrial Aerodynamics*, 29, pp. 409-418.

Matsumoto, M., Saitoh, T., Kitazawa, M., Shirato, H. & Nishizaki, T. (1995) Response characteristics of rain-wind induced vibration of stay-cables of cable-stayed bridges. *Journal of Wind Engineering and Industrial Aerodynamics*, 57, pp. 323-333.

Oron, A., Davis, S.H. & Bankoff, S.G. (1997) Long-scale evolution of thin liquid films. *Reviews of Modern Physics*, 69, 3, pp. 931-980.

Reisfeld, B. & Bankoff, S.G. (1992) Non-isothermal flow of a liquid film on a horizontal cylinder. *Journal of Fluid Mechanics*, 236, pp. 167-196.

Verwiebe, C. & Ruscheweyh, H. (1998) Recent research results concerning the exciting mechanisms of rain-wind-induced vibrations. *Journal of Wind Engineering and Industrial Aerodynamics*, 74-76, pp. 1005-1013.

Xu, Y.L., Zhou, Y., Wang, Z.J. & Wang, L.Y. (2002) Rivulet formation on an inclined cylinder and its effects on the near-wake. *Proc. of ASME-IMECE 2002*, New Orleans, Louisiana, 32173.

Yamaguchi, H. (1990) Analytical study on growth mechanism of rain vibration of cables. *Journal of Wind Engineering and Industrial Aerodynamics*, 33, pp. 73-80.